NAOJ-ALMA-ENG-0017-A
2025-07-28

ALMA Memo 630

Sensitivity with FFT segment overlap in FX-architecture correlator

Kamazaki, T.[1], and Kameno, S.
ALMA project office, National Astronomical Observatory of Japan,
2-21-1 Osawa Mitaka Tokyo 181-8588, Japan
[1] ***kamazaki.takeshi@nao.ac.jp***
2025-07-28

Abstract

We have analytically derived sensitivity changes depending as a function of FFT segment overlap in conventional FX-architecture correlators. The Atacama Compact Array correlator (ACA Correlator) in Atacama Large Millimeter/submillimeter Array (ALMA) is one of the FX-architecture correlators, which computes 2^{20}-point Fast Fourier Transform (FFT) of 4 GSps digital data every 250 μs while overlapping FFT segments with neighboring segments by 48576 samples (= 2^{20}-sample – 4 GSps × 250 μs). The FFT segment overlap was introduced to ensure that the 1 ms integration duration required by ALMA is a multiple of the FFT operating interval. The overlap increases the number of data combinations in the FFT, but it also introduces noise from the overlap regions. This indicates that the sensitivity may depend on the overlap. In this memo, we present an analytical estimate of the sensitivity changes depending on the overlap of FFT segments and verify the estimate with computational simulation.

1. FFT segment overlap of ACA Correlator

FX-architecture (see Section 8 of [1]) is one of the spectroscopy methods of astronomical signals, and the term “FX” is derived from the computational order of the Fourier transform (F) and multiplication (X). In the FX method, the Fourier transform is applied to astronomical signals, and the resulting Fourier products are multiplied by themselves for auto-correlation and by others for cross-correlation. Conventional FX-architecture correlators offer flexible spectral configuration, as they are designed to calculate Fourier products at the highest frequency resolution and output the required multiple frequency ranges with the necessary frequency resolution by selecting and accumulating the highest frequency resolution spectra. On the other hand, it requires more computing and networking resources to achieve the processing of the Fourier transform, which requires $N \log_2 N$ complex multipliers for the N-point Fast Fourier Transform, and the distribution of Fourier products for auto/cross-correlation. However, the rapid growth of digital technology, particularly the development of processing units such as FPGA and

GPU along with high-speed Ethernet, has led to the widespread adoption of the FX method for correlators and spectrometers in radio astronomy.

Atacama Large Millimeter/submillimeter Array (ALMA) consists of 12-m Array and Atacama Compact Array (ACA). The ACA is composed of Total-Power and 7-m Arrays, which take total power and short baseline data for high fidelity imaging in ALMA. ACA Correlator [2] was a FX-architecture correlator, which was responsible for calculating auto and cross correlation spectra of 3-bit 4 GSps digitized receiver signals from ACA. For the compatibility with ALMA Correlator [3] for the 12-m Array, the switching base time of 16 ms in the Walsh switching by 90-degree, and timing critical command executions every 48 ms, ACA Correlator was required to output correlation data with an integration time of 1 ms or 16 ms, depending on the combination of auto and cross correlation. Since ACA Correlator employed FX-architecture with FFT segment length of 2^{20}(=1048576)-sample corresponding to 262.144 μs, it overlapped FFT segment with neighboring segments by 48576 samples and computed 2^{20}-point FFT every 250 μs ($= (1048576 - 48576)/4$ GSps) to realize the integration durations of 1 ms and 16 ms. The overlap can improve the sensitivity of the correlator by increasing the total number of individual data combinations in the FFT. On the other hand, the sensitivity can be reduced due to additional noise from the overlap regions. Thus, we have analytically estimated the sensitivity changes depending on the overlap of FFT segments within a certain time. The analytical results are presented in Section 2 and, for the purpose of confirmation, are compared with computational simulation in Section 3.

2. Analytical estimates of the sensitivity changes depending on FFT segment overlap

We consider the effect of the FFT segment overlap on signal and noise levels in the lag domain in a manner analogous way to Section 8.8.5 of [1] and estimate signal-to-noise ratios (SNRs) as a function of the overlap. Two simple cases are considered in the estimation. The first is a line processing case (hereafter, line observation), where a signal is almost in a spectral channel of the FFT such as a very narrow emission line less than the channel resolution. In this case, all of lag components contribute to both signal and noise in the lag domain. The second is a continuum processing case (hereafter, continuum observation), in which a signal shape is flat in the spectral domain, such as continuum emission. Different from the line observation, the correlation function is a delta-Dirac function in this case, and only zero-lag components contribute to signal and noise. Then, the SNRs of the two cases can be derived by dividing the signal level by the noise level in the lag domain.

The SNRs with and without FFT segment overlap are compared under the condition of same time-series data lengths, corresponding to same observation durations. The following symbols are

defined to represent the data length and the FFT segment overlap.

n_{FFT} : Number of FFT points
N : Number of FFT segments without FFT segment overlap
f : FFT segment overlap factor ($0 \leq f < 1$)

The FFT segment length is defined as "1" for the purpose of simplicity, and the total data length is denoted as "1×*N*" as shown in Figure 1. The FFT segment overlap factor *f* specifies the overlap fraction of two FFT segments, where *f*=0 corresponds to no overlap of neighboring FFT segments, and *f*=0.5 indicates that a half of a segment overlaps with a neighboring segment. The FFT segment overlap factor *f* and the number of FFT segments at FFT segment overlap factor *f* are defined as follows:

$$f \stackrel{\text{def}}{=} \frac{n}{n_{FFT}} \tag{1}$$

where *n* is the number of overlapped samples between two neighboring FFT segments

$$N_f \stackrel{\text{def}}{=} \frac{N-f}{1-f} \tag{2}$$

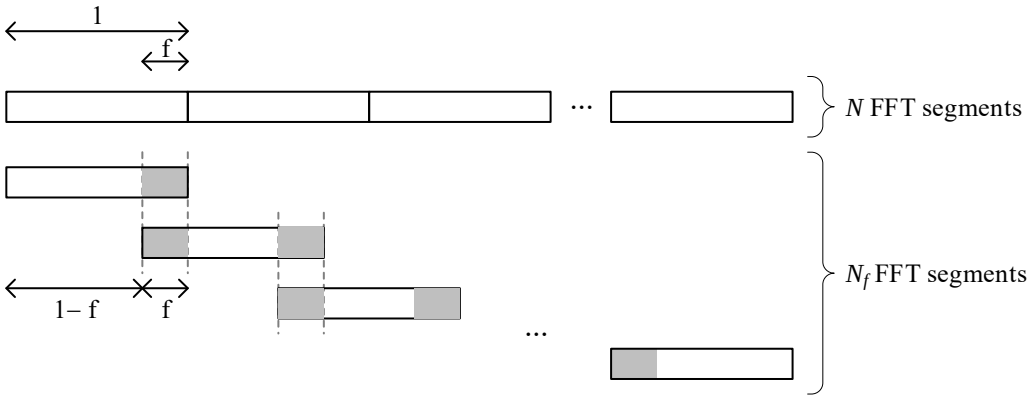

Figure 1. Number of FFT segments at a certain time length.
Total data length is *N* FFT segments. This corresponds to N_f FFT segments at the FFT segment overlap factor *f*.

Signal and noise levels of a FFT segment are denoted as *s* and σ, respectively.

s : Signal level of a FFT segment
σ : Noise level of a FFT segment

Then, SNR is represented as below in the case of N FFT segments without FFT segment overlap.

$$\mathrm{SNR} = \frac{N \cdot s}{\sqrt{N}\sigma} = \sqrt{N}\frac{s}{\sigma} \tag{3}$$

[Signal level]

The total signal level simply depends on the actual number of FFT segments. It is calculated by multiplying the signal level of a single FFT segment with the actual number of FFT segments as shown below. This applies to all overlap factors.

$$N_f s \tag{4}$$

2.1. Number of simultaneous overlaps = 2 ($0<f\leq 1/2$)

First, we consider the case that the number of simultaneous overlaps is 2, corresponding to $0<f\leq 1/2$ as shown in Figure 2.

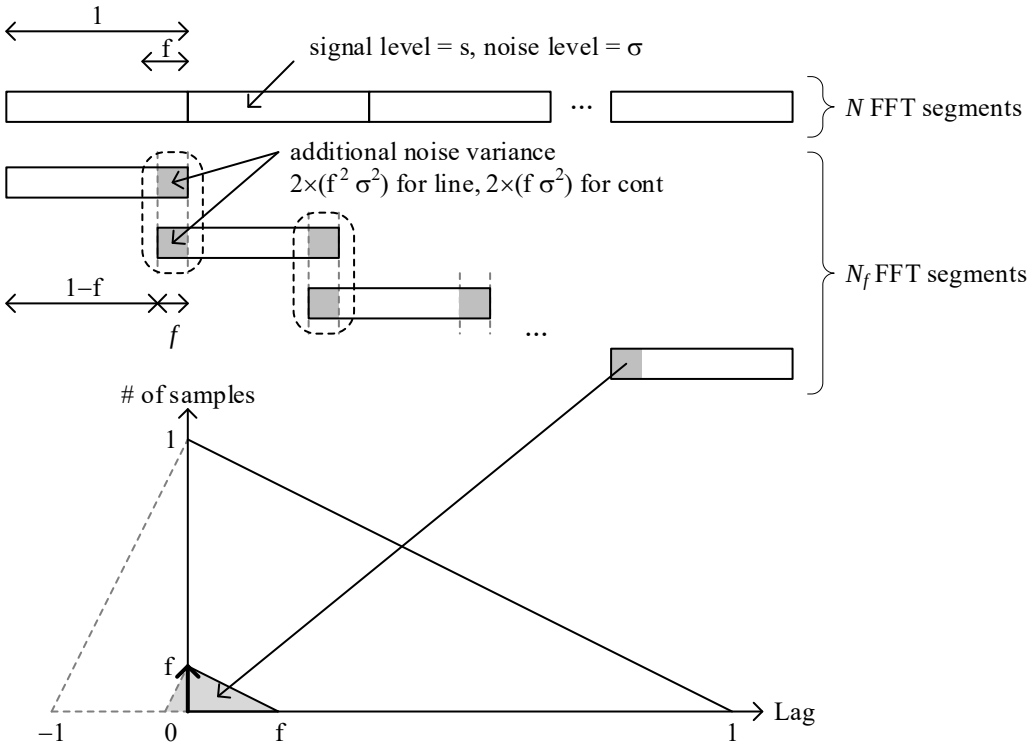

Figure 2. Number of simultaneous overlaps = 2.

Neighboring FFT segments are overlapped by the overlap factor f. The overlap regions of FFT segments are hatched in grey. In the lag domain, the overlap region corresponds to the hatched area in the lower triangle.

Here, we estimate only noise level because signal level is already calculated as denoted in Eq. (4).

[Noise level]

Noise in FFT segment overlap regions is added twice, suggesting that the noise components in these regions are not independent and behave like signals. For the line observation, each of the overlap regions, which are hatched in Figure 2, contains f^2 data, corresponding to a noise variance of $f^2\sigma^2$ in the lag domain. Since there are $(N_f - 1)$ overlap regions, the total noise variance is additionally increased by $2(N_f - 1)f^2\sigma^2$. On the other hand, in the case of the continuum observation, there are f data corresponding to the noise variance of $f\sigma^2$ because only data at zero-lag contributes to it. The total noise variance is increased by $2(N_f - 1)f\sigma^2$. These values are additionally added to $N_f\sigma^2$, which comes from the total number of samples. Hence, the noise levels for the line and continuum observations are represented by Eq. (5) and Eq. (6), respectively.

$$\sigma_{\text{line}} = \sqrt{N_f + 2(N_f - 1)f^2}\ \cdot \sigma \tag{5}$$

$$\sigma_{\text{cont}} = \sqrt{N_f + 2(N_f - 1)f}\ \cdot \sigma \tag{6}$$

[Signal-to-noise ratio]

The SNR is simply represented by the division of the signal level Eq. (4) with the noise level Eq. (5) or Eq. (6).

SNR in the line observation

$$\text{SNR}_{\text{line}} = \frac{N_f}{\sqrt{N_f + 2(N_f - 1)f^2}} \cdot \frac{s}{\sigma} \tag{7}$$

SNR in the continuum observation

$$\text{SNR}_{\text{cont}} = \frac{N_f}{\sqrt{N_f + 2(N_f - 1)f}} \cdot \frac{s}{\sigma} \tag{8}$$

2.2. Number of simultaneous overlaps = 3 ($1/2 < f \leq 2/3$)

Next, we consider the case that the number of simultaneous overlaps is 3, corresponding to $1/2 < f \leq 2/3$ as shown in Figure 3.

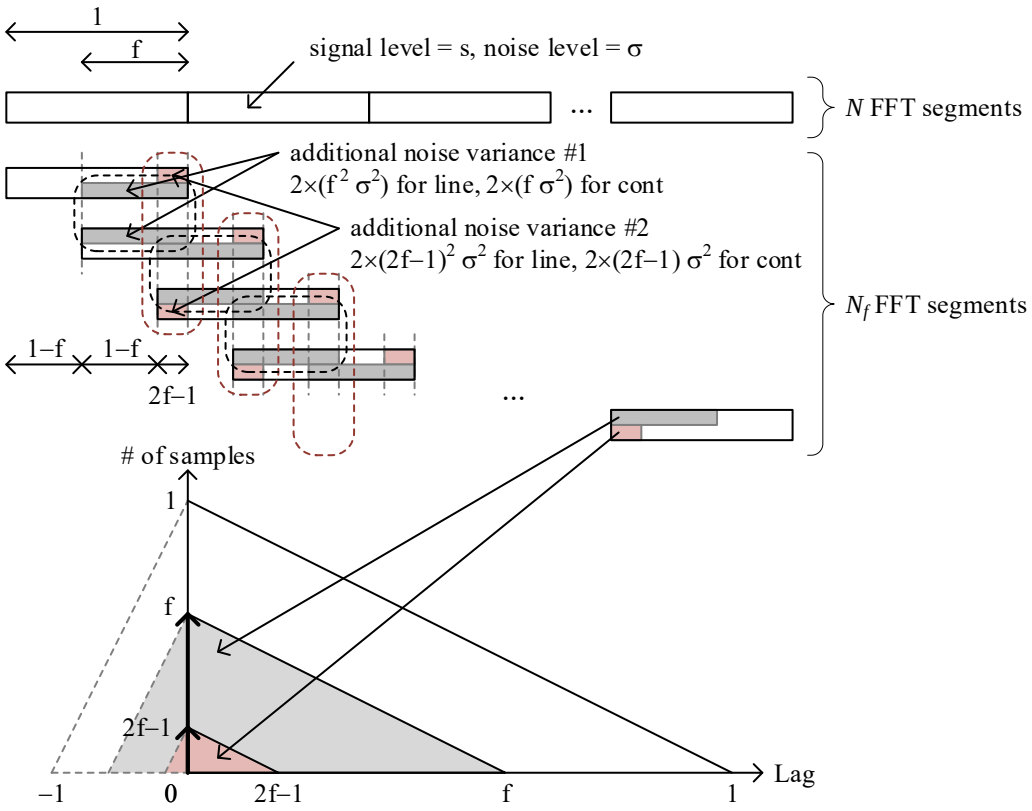

Figure 3. Number of simultaneous overlaps = 3.

Up to three FFT segments simultaneously overlap. The overlap regions are hatched in grey and red in the time and lag domains as well as Figure 2.

[Noise level]

Additional noise (denoted as additional noise variance #1 in Figure 3) from overlap regions of two FFT segments is calculated in the same way as described in Section 2.1. The noise variances are $2(N_f-1)f^2\sigma^2$ and $2(N_f-1)f\sigma^2$ for the line and continuum observations, respectively. In addition, there are (N_f-2) overlap regions of three FFT segments. The additional overlap introduces more noise variances (denoted as additional noise variance #2 in Figure 3) by $2(N_f-2)(2f-1)^2\sigma^2$ for the line observation and $2(N_f-2)(2f-1)\sigma^2$ for the continuum observation. Hence, the noise levels for the line and continuum observations are represented by Eq. (9) and Eq. (10), respectively.

$$\sigma_{\text{line}} = \sqrt{N_f + 2(N_f-1)f^2 + 2(N_f-2)(2f-1)^2}\cdot\sigma \tag{9}$$

$$\sigma_{\text{cont}} = \sqrt{N_f + 2(N_f-1)f + 2(N_f-2)(2f-1)}\cdot\sigma \tag{10}$$

[Signal-to-noise ratio]

The SNR is obtained by dividing the signal level Eq. (4) with the noise level Eq. (9) or Eq. (10) as well as Section 2.1.

SNR in the line observation

$$\mathrm{SNR}_{\mathrm{line}} = \frac{N_f}{\sqrt{N_f + 2(N_f-1)f^2 + 2(N_f-2)(2f-1)^2}} \cdot \frac{s}{\sigma} \tag{11}$$

SNR in the continuum observation

$$\mathrm{SNR}_{\mathrm{cont}} = \frac{N_f}{\sqrt{N_f + 2(N_f-1)f + 2(N_f-2)(2f-1)}} \cdot \frac{s}{\sigma} \tag{12}$$

2.3. Number of simultaneous overlaps = 4 (2/3<*f*≤3/4)

Similarly, we consider the case that the number of simultaneous overlaps is 4, corresponding to 2/3<*f*≤3/4 as shown in Figure 4.

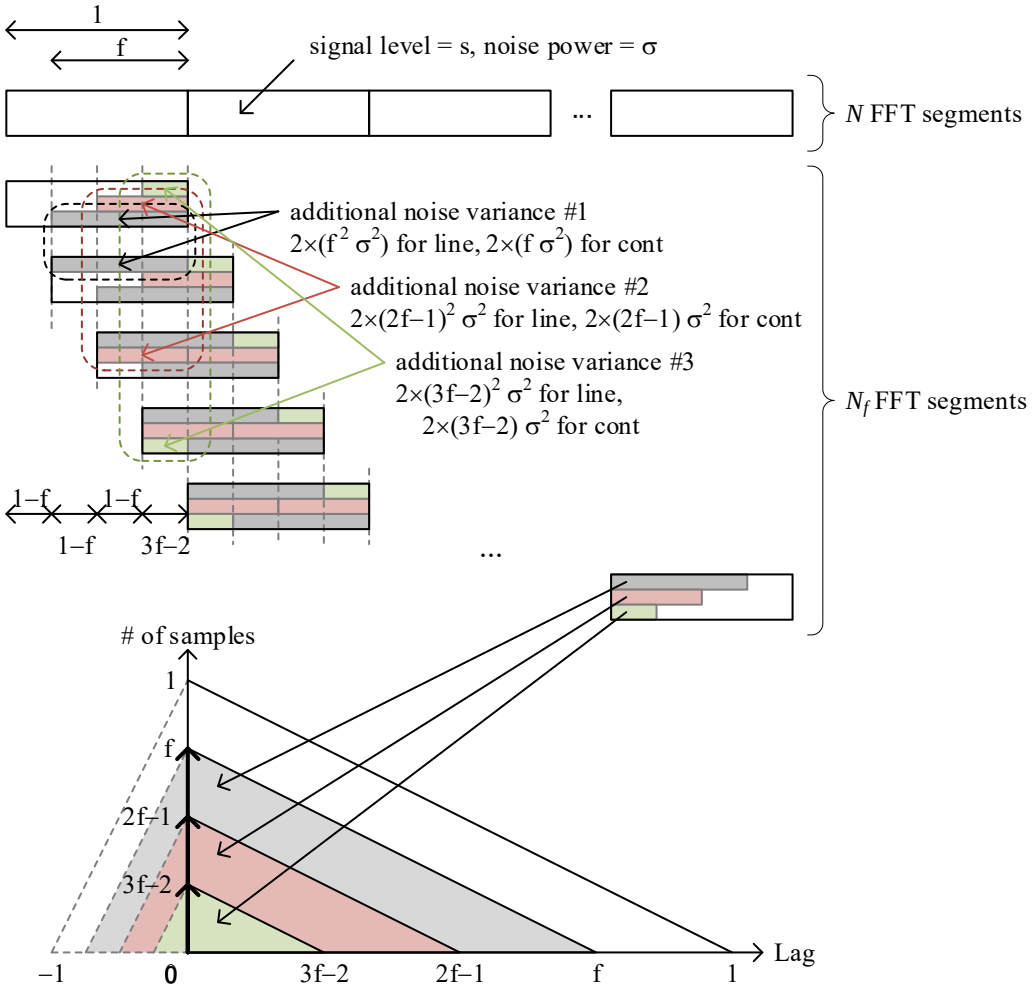

Figure 4. Number of simultaneous overlaps = 4.

Up to four FFT segments overlap. The overlap regions are hatched in grey, red, and green as well as Figure 2.

[Noise level]

Additional noise is calculated in the same way as described in Section 2.1 and Section 2.2. In this case, there are $(N_f - 3)$ regions, where four FFT segments are overlapped as shown in Figure 4, in addition to two-segment and three-segment overlap regions. The four-segment overlap regions add noise variances (denoted as additional noise variance #3 in Figure 4) of $2(N_f - 3)(3f - 2)^2\sigma^2$ and $2(N_f - 3)(3f - 2)\sigma^2$ in the line and continuum observations, respectively. Hence, the noise levels for the line and continuum observations are represented by Eq. (13) and Eq. (14), respectively.

$$\sigma_{\text{line}} = \sqrt{N_f + 2(N_f - 1)f^2 + 2(N_f - 2)(2f - 1)^2 + 2(N_f - 3)(3f - 2)^2} \cdot \sigma \quad (13)$$

$$\sigma_{\text{cont}} = \sqrt{N_f + 2(N_f - 1)f + 2(N_f - 2)(2f - 1) + 2(N_f - 3)(3f - 2)} \cdot \sigma \quad (14)$$

[Signal-to-noise ratio]

The SNR is obtained by dividing the signal level Eq. (4) with the noise level Eq. (13) or Eq. (14).

SNR in the line observation

$$\text{SNR}_{\text{line}} = \frac{N_f}{\sqrt{N_f + 2(N_f - 1)f^2 + 2(N_f - 2)(2f - 1)^2 + 2(N_f - 3)(3f - 2)^2}} \cdot \frac{s}{\sigma} \quad (15)$$

SNR in the continuum observation

$$\text{SNR}_{\text{cont}} = \frac{N_f}{\sqrt{N_f + 2(N_f - 1)f + 2(N_f - 2)(2f - 1) + 2(N_f - 3)(3f - 2)}} \cdot \frac{s}{\sigma} \quad (16)$$

2.4. Number of simultaneous overlaps = *F*

Finally, we consider the general case that the number of simultaneous overlaps is *F*.

[Noise level]

From the analysis of the cases of *F*=2, 3, and 4, it is evident that an additional term is included in the noise variance when *F* increased from *p* to *p*+1.

Additional noise variance in the line observation

$$\{2(N_f - p)\{p(f-1)+1\}^2\}\sigma^2 \tag{17}$$

Additional noise variance in the continuum observation

$$\left\{2(N_f - p)\{p(f-1)+1\}\right\}\sigma^2 \tag{18}$$

Then, the noise level is represented as follows:

Noise level in the line observation

$$\begin{aligned}\sigma_{\text{line}} &= \sqrt{N_f + 2(N_f-1)f^2 + 2(N_f-2)(2f-1)^2 + 2(N_f-3)(3f-2)^2 + \cdots}\cdot\sigma \\ &= \sqrt{N_f + \sum_{p=1}^{F-1} 2(N_f-p)\{p(f-1)+1\}^2}\cdot\sigma \\ &= \sqrt{-N_f + \sum_{p=0}^{F-1} 2(N_f-p)\{p(f-1)+1\}^2}\cdot\sigma\end{aligned} \tag{19}$$

Noise variance in the continuum observation

$$\begin{aligned}\sigma_{\text{cont}} &= \sqrt{N_f + 2(N_f-1)f + 2(N_f-2)(2f-1) + 2(N_f-3)(3f-2) + \cdots}\cdot\sigma \\ &= \sqrt{N_f + \sum_{p=1}^{F-1} 2(N_f-p)\{p(f-1)+1\}}\cdot\sigma \\ &= \sqrt{-N_f + \sum_{p=0}^{F-1} 2(N_f-p)\{p(f-1)+1\}}\cdot\sigma\end{aligned} \tag{20}$$

[Signal-to-noise ratio]

Finally, the SNR in the general case is represented as follows:

SNR in the line observation

$$\text{SNR}_{\text{line}} = \frac{N_f}{\sqrt{-N_f + \sum_{p=0}^{F-1} 2(N_f-p)\{p(f-1)+1\}^2}}\cdot\frac{s}{\sigma} \tag{21}$$

SNR in the continuum observation

$$\text{SNR}_{\text{cont}} = \frac{N_f}{\sqrt{-N_f + \sum_{p=0}^{F-1} 2(N_f-p)\{p(f-1)+1\}}}\cdot\frac{s}{\sigma} \tag{22}$$

2.5. Sensitivity changes

Figure 5 shows SNR plots represented by Eq. (21) and Eq. (22). In the line observation, the SNR simply increases with the FFT segment overlap factor f. This can be explained by increased number of individual combinations of data in FFT processing. On the other hand, in the continuum observation, the SNR is 1.0 when $1/f$ is $n/(n+1)$ $(n = 0, 1, 2, \dots)$, otherwise it is lower than 1.0. This SNR behavior in the continuum observation can be attributed to overlap ways of FFT segments.

In the case that is $1/f \neq n/(n+1)$ $(n = 0, 1, 2, \dots)$, FFT segments are overlapped with other segments with gaps. For example, at f=0.046, a segment overlaps with two neighboring segments at both 4.6% edges of the segment, and its remaining range never overlaps with the other segments. This unequal overlap results in unequal weights within FFT segments, which increase noise level. Furthermore, the overlap of FFT segments does not increase the number of independent zero-lag components. Consequently, the SNR is lower than 1.0 at $1/f \neq n/(n+1)$ $(n = 0, 1, 2, \dots)$. For example, in the case of 0<f<1/2, Eq. (8) is expressed as below:

$$\mathrm{SNR}_{\mathrm{cont}} = \frac{\sqrt{N}}{\sqrt{(1-f)(1+2f)}} \cdot \frac{s}{\sigma} \quad (N \gg 1)$$

The denominator is 1 at f=0, 1/2. It is larger than 1 at 0<f<1/2, and there is the maximum sensitivity loss occurs at f=0.25.

In the case that is $1/f = n/(n+1)$ $(n = 0, 1, 2, \dots)$, FFT segments overlap with each other without the presence of the gaps, and there is no difference in the number of overlaps within a given segment. Consequently, signal and noise components are equally accumulated in-phase by the overlaps. As a result, the SNRs remain at 1.0 in the case of $1/f = n/(n+1)$ $(n = 0, 1, 2, \dots)$.

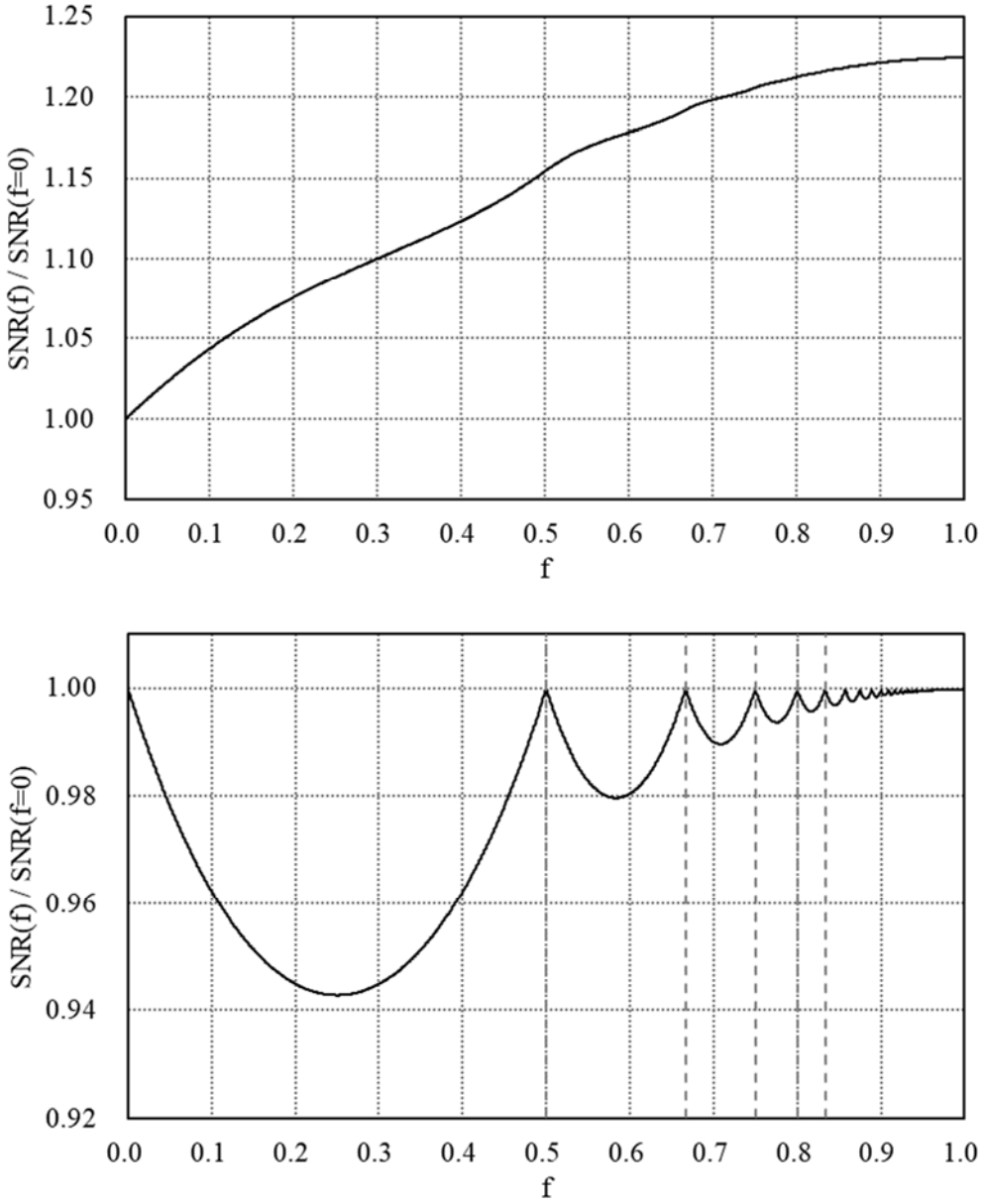

Figure 5. Sensitivity changes with the FFT segment overlap factor *f*.

The upper and lower plots show the sensitivity changes for the line and continuum observations, respectively, depending on the FFT segment overlap factor *f*. The vertical dashed lines indicate *f*=1/2, 2/3, 3/4, 4/5, and 5/6, where the overlap number increases by +1.

3. Computational simulation

In the previous section, we have derived the two equations, Eq. (21) and Eq. (22), representing SNRs depending on the FFT segment overlap factor in the line and continuum observations. Figure 5 plots the SNR changes that correspond to sensitivity changes with the overlap factor. In this section, we estimate the sensitivity changes using the Monte Carlo method to verify Eq. (21),

Eq. (22), and Figure 5.

Our calculation steps are as follows:

Step 1. Two independent time-series data sets with Gaussian noise are generated computationally, each of which has a mean of 0.0 and a standard deviation of 0.8. Another time-series data set is added to them for three different cases, which are (a) line observation of a sin wave, (b) line observation of correlated Gaussian noise with a narrow-line spectrum, and (c) continuum observation of correlated Gaussian noise with a flat spectrum.

The same FFT segment length of 1048576 (= 2^{20}) is adopted as that used by ACA Correlator, and the total data length of 419430400 corresponds to 400 FFT segments without FFT segment overlap. To ensure N_f in Eq. (2) becomes an integer, the data length is slightly adjusted for each overlap factor. There are slight differences of less than 0.1 % in data lengths among the different overlap factors, but they are negligible in the estimate of the SNRs.

Step 2. The time-series data are divided by the FFT segment length with segment overlap specified by the overlap factor. Then, auto- and cross-power spectra are calculated for each FFT segment and averaged over all segments. The cross-power spectra are normalized by the corresponding auto-power spectra to convert them to correlation coefficients. Additionally, spectral channel averaging by 1024-channel is applied in the continuum observation.

Step 3. The signal and noise levels are estimated from the normalized cross-power spectra.

Step 4. 100 spectra are calculated for each overlap factor of each case, and signal and noise levels derived from them are averaged to estimate a SNR.

3.1. Line observation of a sine wave

Figure 6 shows an example of cross-power spectra of a sine wave. A sine wave with an amplitude of 1.0 and a frequency of a quarter of FFT-point was adopted for use at Step 1 of the calculation steps.

Table 1 presents the overlap factor *f*, number of overlaps, total number of samples, SNR, and SNR normalized by the SNR without FFT segment overlap (f=0). You can see that the normalized SNRs are well consistent with each other between the simulation and analytical results. This consistency is also evident in Figure 7, which plots the normalized SNRs of the simulation results on the normalized SNRs calculated from Eq. (21).

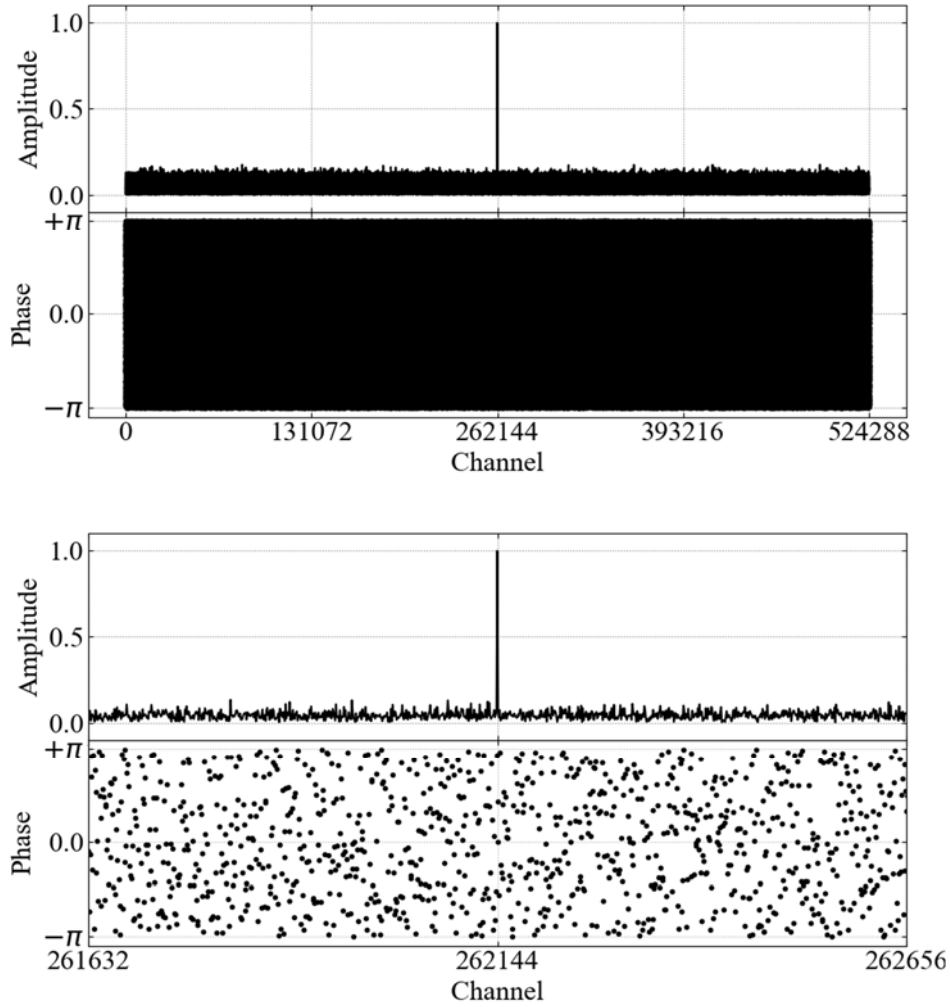

Figure 6. Cross-power spectra of a sine wave.

(Upper) Amplitude and phase plots of a cross-power spectrum of the sine waves at the FFT segment overlap factor f=0. (Lower) Zoomed-in views of the sine spectrum of the upper plots. The spectral center is located at 262144-channel. A signal level is the peak amplitude, and a noise level is a standard deviation in the two ranges of [0 – 262127] and [262160 – 524287] channels.

Table 1. Comparison of the normalized SNRs between simulation and analytical results in the line observation toward a sin wave

Overlap factor "f"	# of overlaps	# of FFT segments (total samples *1) [×100]	SNR [$\times 10^2$]	SNR[f]/SNR[f=0]	
				Simulation	Analysis Eq. (21)
0.000	1	400 (419430400)	4.313	1.000	1.000

0.046	2	419 (419048576)	4.405	1.021	1.022
0.125	2	457 (419430400)	4.540	1.053	1.053
0.250	2	533 (419430400)	4.695	1.089	1.089
0.375	2	639 (419168256)	4.818	1.117	1.117
0.450	2	726 (419168401)	4.905	1.137	1.137
0.500	2	799 (419430400)	4.980	1.155	1.155
0.560	3	907 (419053420)	5.050	1.171	1.171
0.625	3	1065 (419430400)	5.101	1.183	1.183
0.667	3	1197 (419081672)	5.139	1.191	1.192
0.710	4	1376 (419169576)	5.174	1.200	1.200
0.750	4	1597 (419430400)	5.201	1.206	1.206
0.770	5	1735 (419242558)	5.213	1.209	1.209
0.875	8	3193 (419430400)	5.261	1.220	1.220
0.990	100	39900 (419429490)	5.281	1.224	1.224

*1 The number of samples is slightly different depending on the FFT segment overlap factor. Since the differences are less than 0.1 %, the normalized SNRs listed in the table are little affected by them.

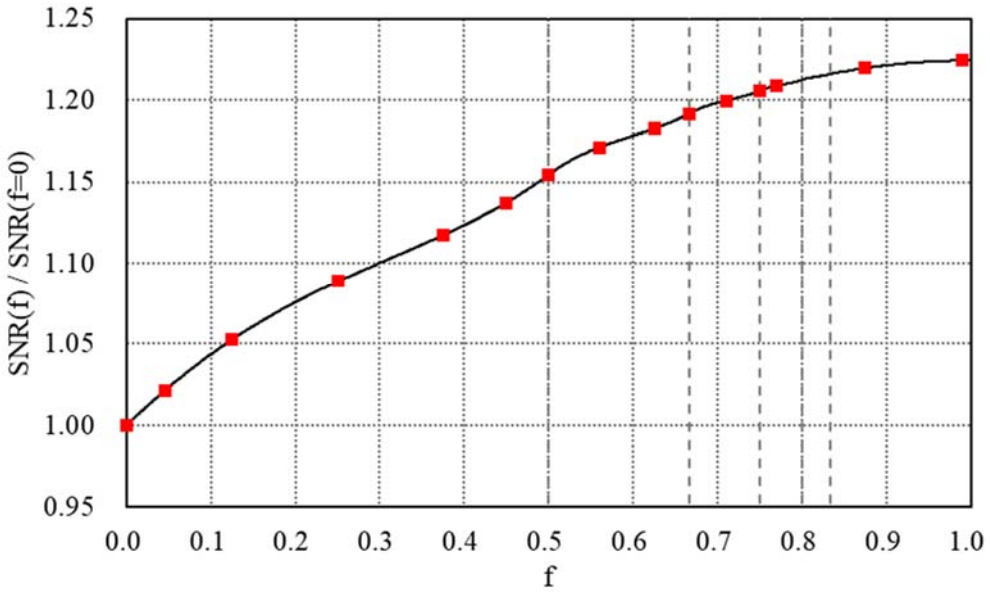

Figure 7. Normalized SNRs of the simulation plotted on the line of normalized SNRs calculated from Eq. (21) in the line observation of a sine wave.

The red boxes indicate the simulation results, and the solid line is the analytical result. The vertical dashed lines indicate f=1/2, 2/3, 3/4, 4/5, and 5/6, where the number of the overlap increases by +1.

3.2. Line observation of correlated Gaussian noise with a narrow-line spectrum

Figure 8 shows an example of a cross-power spectrum of correlated Gaussian noise with a narrow spectrum. The narrow-line spectrum is generated by filtering Gaussian noise with a mean of 0.0 and a standard deviation of 0.8 using a FIR bandpass filter and is used at Step 1 of the calculation steps.

Table 2 lists comparison results between simulation and analytical results in the line as well as Table 1. The normalized SNRs are consistent between the two results as also shown in Figure 9.

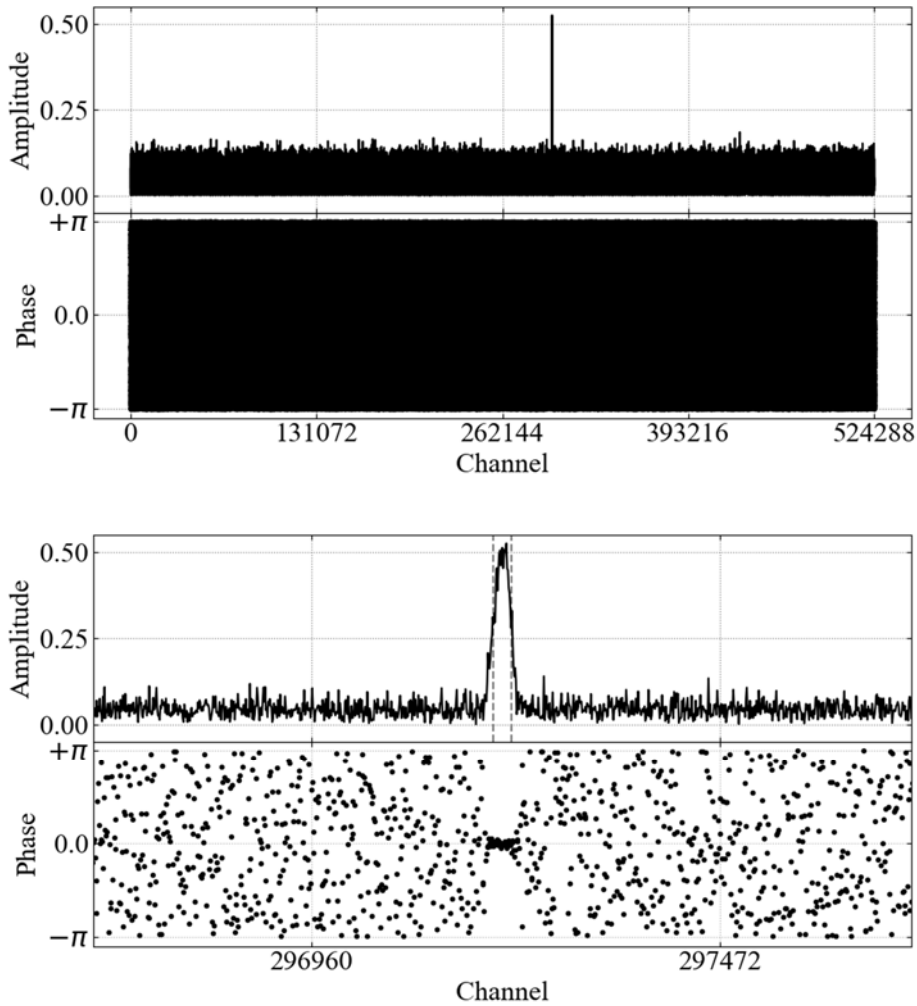

Figure 8. Cross-power spectra of correlated Gaussian noise with a narrow spectrum.

(Upper) Amplitude and phase plots of the correlated Gaussian noise with a narrow spectrum at the FFT segment overlap factor f=0. (Lower) Zoomed-in views of the narrow spectrum of the upper plots. The spectral center is located at 297199-channel, and its FWHM is 22-channel indicated by two dashed vertical lines. The amplitudes within the FWHM range are

averaged to estimate a signal level, and a noise level is a standard deviation in the two ranges of [0 – 296959] and [297472 – 524287] channels.

Table 2. Comparison of the normalized SNRs between simulation and analytical results in the line observation toward correlated Gaussian noise with a narrow spectrum

Overlap factor "*f*"	# of overlaps	# of FFT segments (total samples *1) [×100]	SNR [$\times 10^2$]	SNR[f]/SNR[f=0]	
				Simulation	Analysis Eq. (21)
0.000	1	400 (419430400)	1.854	1.000	1.000
0.046	2	419 (419048576)	1.892	1.021	1.022
0.125	2	457 (419430400)	1.951	1.052	1.053
0.250	2	533 (419430400)	2.018	1.088	1.089
0.375	2	639 (419168256)	2.070	1.116	1.117
0.450	2	726 (419168401)	2.108	1.137	1.137
0.500	2	799 (419430400)	2.139	1.154	1.155
0.560	3	907 (419053420)	2.170	1.170	1.171
0.625	3	1065 (419430400)	2.192	1.182	1.183
0.667	3	1197 (419081672)	2.208	1.191	1.192
0.710	4	1376 (419169576)	2.224	1.199	1.200
0.750	4	1597 (419430400)	2.235	1.205	1.206
0.770	5	1735 (419242558)	2.240	1.208	1.209
0.875	8	3193 (419430400)	2.260	1.219	1.220
0.990	100	39900 (419429490)	2.269	1.224	1.224

*1 The number of samples are slightly different depending on the FFT segment overlap factor as well as Table 1.

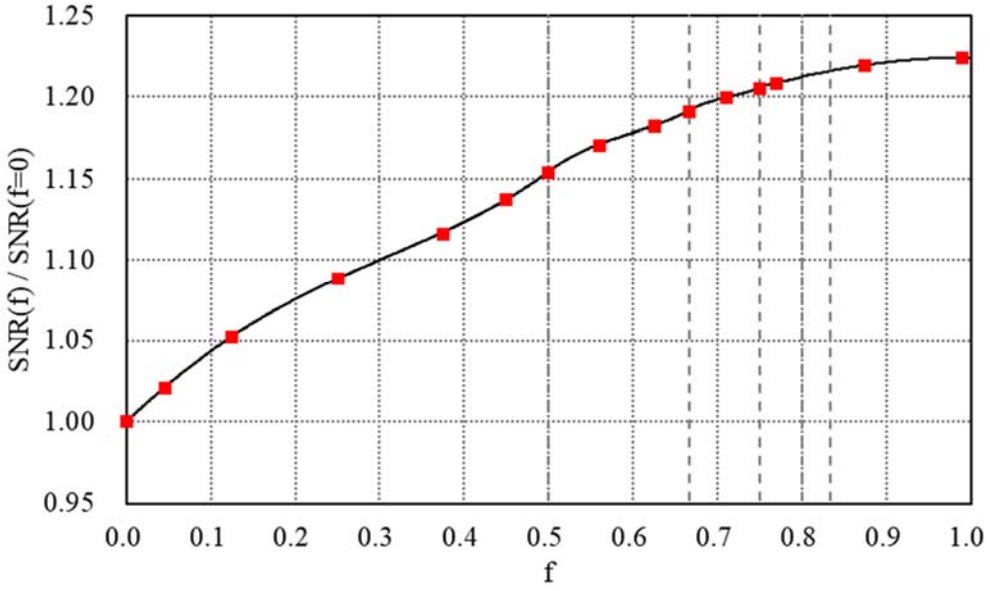

Figure 9. Normalized SNRs of the simulation plotted on the line of normalized SNRs calculated from Eq. (21) in the line observation of correlated Gaussian noise with a narrow spectrum.

The red boxes indicate the simulation results, and the solid line is the analytical result. The vertical dashed lines are same as those in Figure 7.

3.3. Continuum observation of correlated Gaussian noise with a flat spectrum

Figure 10 shows an example of a cross-power spectrum of correlated Gaussian noise with a flat spectrum. At Step 1 in the calculation steps, additional time-series data set of Gaussian noise with a mean of 0.0 and a standard deviation of 0.8 is used to generate correlated Gaussian noise with a flat spectrum, whose correlation coefficient is 0.5.

Table 3 lists comparison results between simulation and analytical results in the continuum as well as Table 1. The normalized SNRs are consistent between the two results as shown in Figure 11, which plots the normalized SNRs of the simulation results on the normalized SNRs calculated from Eq. (22).

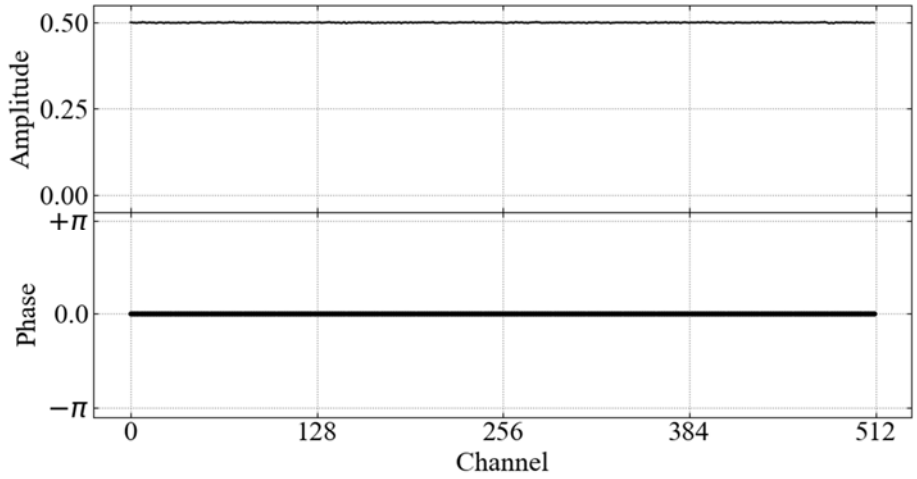

Figure 10. Cross-power spectrum of correlated Gaussian noise with a flat spectrum.

Amplitude and phase plots of the cross-power spectrum normalized by its corresponding auto-power spectra at the FFT segment overlap factor f=0. Signal and noise levels are estimated from mean and standard deviation of spectral amplitudes, respectively.

Table 3. Comparison of the normalized SNRs between simulation and analytical results in the continuum observation.

Overlap factor "f"	# of overlaps	# of FFT segments (total samples *1) [×100]	SNR [$\times 10^3$]	SNR[f]/SNR[f=0]	
				Simulation	Analysis Eq. (22)
0.000	1	400 (419430400)	6.076	1.000	1.000
0.046	2	419 (419048576)	5.947	0.979	0.980
0.125	2	457 (419430400)	5.814	0.957	0.956
0.250	2	533 (419430400)	5.724	0.942	0.943
0.375	2	639 (419168256)	5.813	0.957	0.956
0.450	2	726 (419168401)	5.949	0.979	0.978
0.500	2	799 (419430400)	6.075	1.000	1.000
0.560	3	907 (419053420)	5.960	0.981	0.981
0.625	3	1065 (419430400)	5.978	0.984	0.985
0.667	3	1197 (419081672)	6.072	0.999	1.000
0.710	4	1376 (419169576)	6.017	0.990	0.990
0.750	4	1597 (419430400)	6.074	1.000	1.000
0.770	5	1735 (419242558)	6.036	0.993	0.994

0.875	8	3193 (419430400)	6.074	1.000	1.000
0.990	100	39900 (419429490)	6.074	1.000	1.000

*1 The number of samples are slightly different depending on the FFT segment overlap factor as well as Table 1.

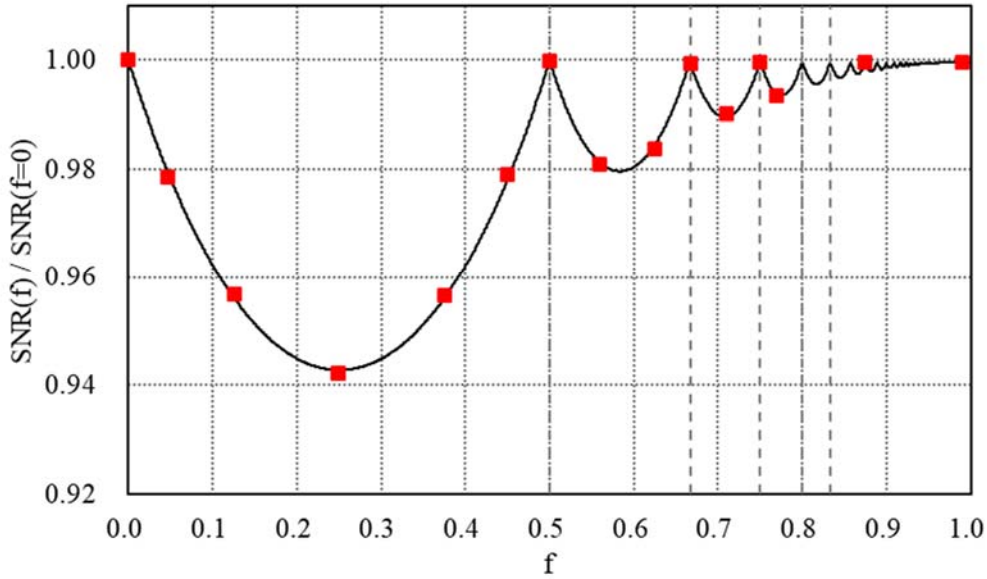

Figure 11. Normalized SNRs of the simulation plotted on the line of normalized SNRs calculated from Eq. (22) in the continuum observation of correlated Gaussian noise with a flat spectrum.

The red boxes indicate the simulation results, and the solid line is the analytical result. The vertical dashed lines indicate f=1/2, 2/3, 3/4, 4/5, and 5/6, where the number of the overlaps increases by +1.

4. Summary

We have analytically derived the equations representing the impact of FFT segment overlap on the sensitivity of FX-architecture correlators. The results indicate that an increase in the FFT segment overlap factor f leads to sensitivity improvement in the line observation. This is due to the increase in the number of independent combinations of time-series data as the overlap factor increases. In contrast, the sensitivity in the continuum observation remains 1.0 at $1/f = n/(n+1)$ $(n = 0, 1, 2, \dots)$, otherwise it decreases. The continuum observation simply accumulates spectra in time and frequency, therefore, the FFT segment overlap does not increase the amount of information, and on the contrary, the overlap can increase noise due to unequally overlapped segments. We have also compared the analytical results with the simulation results calculated using the Monte Carlo method. The analytical and simulation results agree well with

each other, confirming that the equations represent the sensitivity changes depending on the FFT segment overlap.

We would like to acknowledge the reviewer for constructive comments and suggestions which improve our paper. We are grateful to Satoru Iguchi for his constructive comments.

References

[1] Thompson, A. R., Moran, J. M., and Swenson, G. W. Jr., Interferometry and Synthesis in Radio Astronomy Third Edition, Springer Open, 2017

[2] Kamazaki, T., Okumura, K. S., Chikada, Y., Okuda, T., Kurono, Y., Iguchi, S., Mitsuishi, S., Murakami, Y., Nishimuta, N., Mita, H., and Sano, R., 2012, “Digital Spectro-Correlator System for the Atacama Compact Array of the Atacama Large Millimeter/Submillimeter Array”, PASJ, 64, 29

[3] Escoffier, R. P., Comoretto, G., Webber, J. C., Baudry, A., Broadwell, C. M., Greenberg, J. H., Treacy, R. R., Cais, P., Quertier, B., Camino, P., Bos, A., and Gunst, A. W., 2007, “The ALMA correlator”, A&A, 462, 801

[4] Okumura, S. K., Chikada, Y., Momose, M., and Iguchi, S., 2001, “Feasibility Study of the Enhanced Correlator for Three-Way ALMA”, ALMA Memo 350

Appendix A Sensitivity comparison between FX and XF correlators

We have compared sensitivity with spectral channel averaging between FX and XF correlators. In the comparison, SNRs of a FX correlator with FFT segment overlap factor *f*=0.990 are substituted for those of a XF correlator. It can be reasonably assumed that the data density of the FX correlator in the lag domain is approximately equivalent to that of a XF correlator, given that each FFT segment is well overlapped with neighboring FFT segments 100 times at *f*=0.990.

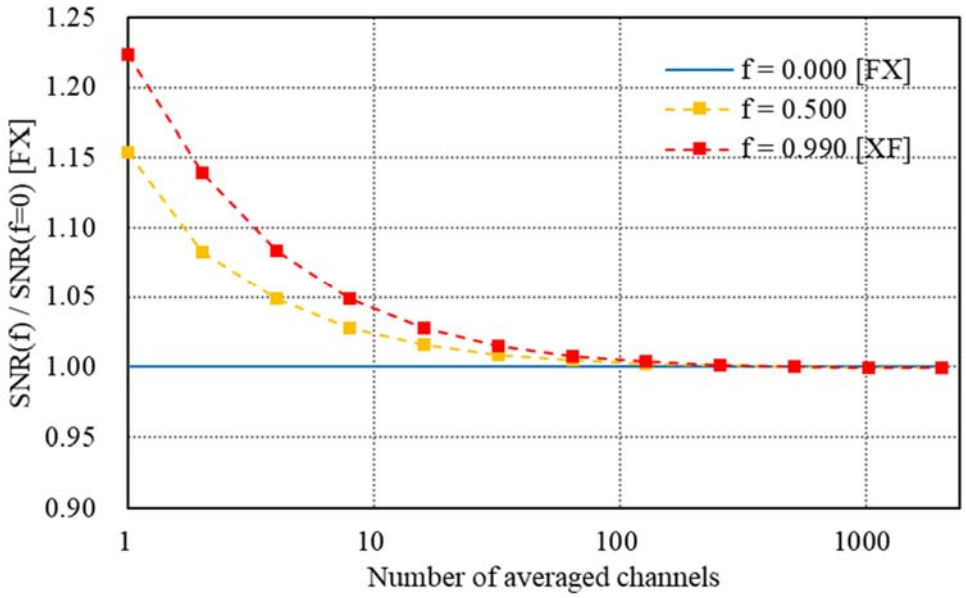

Figure 12. Sensitivity comparison between FX and XF correlators depending on spectral channel averaging and FFT segment overlap without gaps.

Red and orange boxes show the relative SNRs of the XF correlator (the FX correlator with f=0.990) and the FX correlator (f=0.500) against the FX correlator (f=0.000) indicated by a blue line, respectively, at each number of averaged channels.

Figure 12 shows the relative SNRs between the FX and XF correlators as a function of the number of averaged channels, where correlated Gaussian noise with a flat spectrum is used to estimate the SNRs of each correlator. The plot for *f*=0.990 corresponding to the XF correlator is consistent with Figure 6 in ALMA Memo 350 [4] and approaches 1.0 as the number of averaged channels increases. The plot for *f*=0.500 is more closely aligned with the *f*=0.990 plot than the *f*=0.000 plot and approaches 1.0 at a larger number of averaged channels as well. These results indicate that the spectral channel averaging as well as the FFT segment overlap can improve the sensitivity of the FX correlator, approaching that of the XF correlator. For example, 2-channel averaging can increase the sensitivity by about 7% $(1/1.22 \rightarrow 1/1.14)$ compared to non-channel averaging. On the other hand, the sensitivity improvement is about 15% using FFT segment overlap from

f=0.000 to *f*=0.500. The improvement by the spectral channel averaging can be explained by the fact that the channel averaging in the spectral domain is equivalent to multiplication of a sinc function in the lag domain. Since the sinc function narrows with an increasing number of averaged channels, the SNR is dominated by lag zero values, which are nearly equivalent to SNR in the continuum observation.

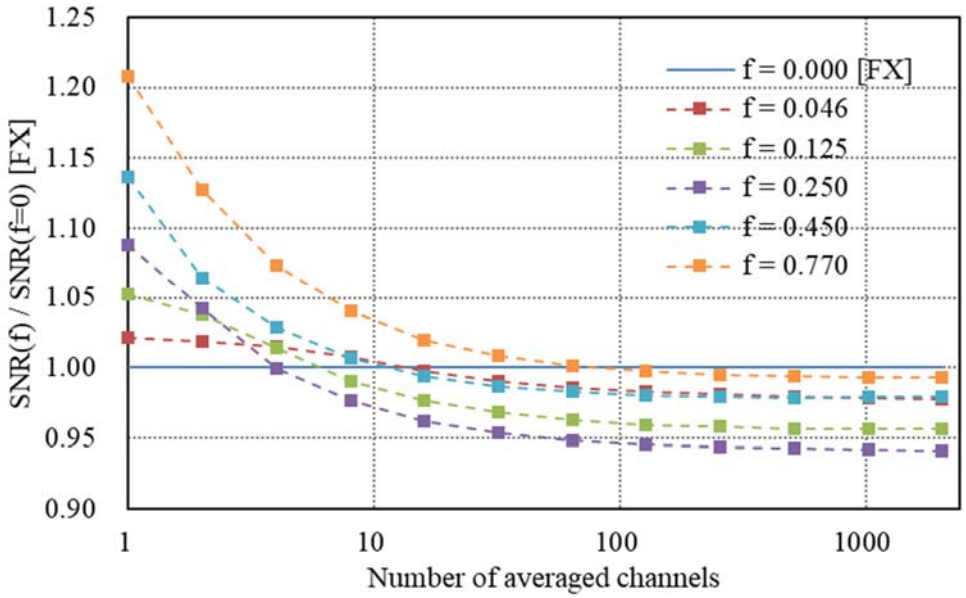

Figure 13. Sensitivity comparison between FX and XF correlators depending on spectral channel averaging and FFT segment overlap with gaps.
Boxes with different colors show the relative SNRs of the FX correlator with different overlap factors *f*=0.046, 0.125, 0.250, 0.450, and 0.770 against the FX correlator (*f*=0.000) indicated by a blue line at each number of averaged channels.

In Figure 13, we additionally show the relative SNRs of the FX correlator with some of the overlap factors, where the normalized SNRs are less than 1.0 in Figure 11, as a function of the number of averaged channels. Figure 13 shows that the sensitivity can improve with the spectral channel averaging and/or FFT segment overlap as well as Figure 12, however, it also shows that wide channel averaging like the continuum observation can reduce the sensitivity as predicted from the discussion about the continuum observation in Section 2.5.

Figure 14 summarizes the behaviors shown in Figure 12 and Figure 13. It plots the relative SNRs of the FX correlator with a segment overlap factor against the XF correlator at each number of averaged channels. The relative SNRs distribute between the red and blue lines corresponding to the line and continuum observations and basically approach to 1.0 at wider spectral channel

averaging and/or larger FFT segment overlap.

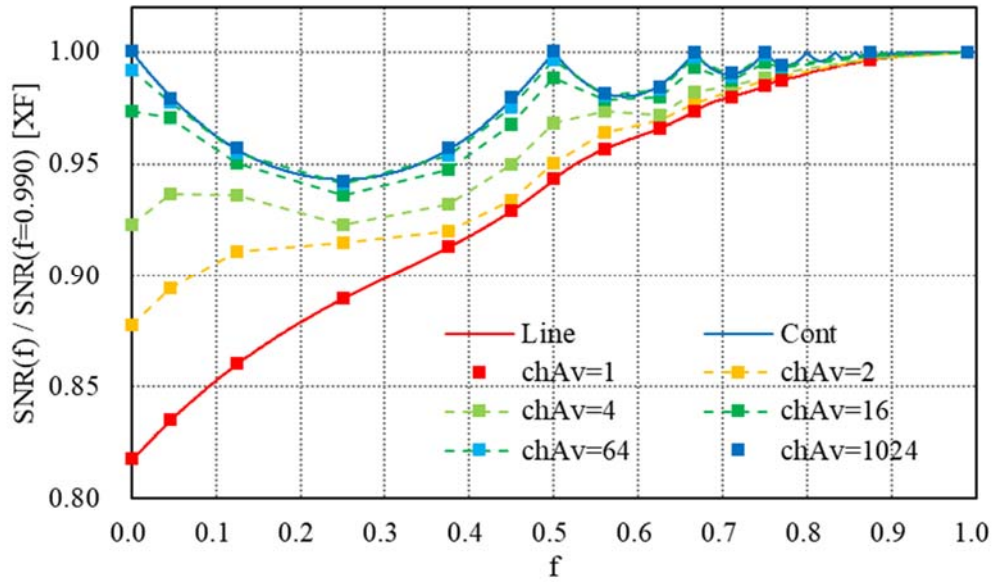

Figure 14. Relative sensitivity of the FX correlator against the XF correlator.
Lines and boxes show the relative SNRs of the FX correlator against the XF correlator (the FX correlator with f=0.990). Red and blue lines are the analytically derived relative SNRs for the line and continuum observations, respectively. Boxes in different colors indicate relative SNRs with different numbers of average channels (chAv=1, 2, 4, 16, 64, and 1024).